January 1989 LIDS-P-1843

A HIERARCHICAL ALGORITHM FOR LIMITED-ANGLE RECONSTRUCTION

Jerry L. Prince and Alan S. Willsky

Laboratory for Information and Decision Systems
Department of Electrical Engineering,
Massachusetts Institute of Technology, Cambridge, MA 02139

Abstract

In this paper, we describe and demonstrate a hierarchical reconstruction algorithm for use in noisy and limited-angle or sparse-angle tomography. The algorithm estimates the object's mass, center of mass, and convex hull from the available projections, and uses this information, along with fundamental mathematical constraints, to estimate a full set of smoothed projections. The mass and center of mass estimates are made using a maximum likelihood (ML) estimator derived from the principles of consistency of the Radon transform. The convex hull estimate is produced by first estimating the positions of support lines of the object from each available projection and then estimating the overall convex hull using ML techniques or maximum *a posteriori* (MAP) techniques. Estimating the position of two support lines from a single projection is accomplished using either a generalized likelihood ratio technique for estimating jumps in linear systems, or a support-width penalty method that uses Akaike's model order estimation technique. We show results for a simulated object in a variety of measurement situations and for several model parameters and discuss several possible extensions to the work.

I. Introduction

It has been demonstrated in the literature that prior geometric information about either the object or its 2-D Radon transform can significantly improve reconstructions when the tomographic imaging system has both a restricted view and a low signal to noise ratio (see [1]). Often, however, it is not clear how this information may be reliably determined, *a priori*. This paper describes a hierarchical algorithm that first estimates the mass, center of mass, and convex hull of the object, and then uses this information in a second stage, described in [2], which estimates a complete image of the 2-D Radon transform of the object — called a *sinogram* — using a fast primal-dual optimization technique. The object estimate is produced using convolution backprojection (CBP) applied to the estimated sinogram.

The 2-D Radon transform is given by

$$g(t,\theta) = \int_{-\infty}^{\infty} f(x)\delta(t-\omega^{\mathrm{T}}x)dx\,, \qquad (1)$$

where $\omega = [\cos\theta \;\; \sin\theta]^{\mathrm{T}}$, $\delta(\cdot)$ is the Dirac delta function, and $f(x)$ is a real function defined on the plane and is assumed to be zero outside the disk of radius T centered at the origin (see Fig. 1). For a particular θ the function $g(t,\theta)$ is a function of t, and is called a *projection*. When a large number of high quality measurements of $g(t,\theta)$ for $t \in [-T,T]$ and $\theta \in [0,\pi)$ are available, then a high quality reconstruction may be obtained using CBP or other methods (see [3]). However, in applications where the measurements are noisy and may be available over a limited range or sparse set of angles, the conventional methods are not adequate.

In this paper we assume that the observations are given by

$$y(t_i,\theta_j) = g(t_i,\theta_j) + n(t_i,\theta_j) \qquad (2)$$

where the indices $i \in \{1,\ldots,n_d\}$ and $j \in \{1,\ldots,n_v\}$ give a point in the regular rectangular lattice in the domain $[-T,T] \times [0,\pi)$. The noise samples $n(t_i,\theta_j)$ are zero-mean white Gaussian random variables, independent between lattice sites.

Many methods have been proposed to address the problems of noisy or missing data with varying degrees of success (see [4] and references). In [2], we proposed a projection-space method that successfully deals with both problems simultaneously. A disadvantage of this algorithm, which is shared by others in the literature, is that it requires particular prior knowledge in order to produce its estimate. In this case, the algorithm requires knowledge of the object's mass, center of mass, and convex support. This paper describes a method to estimate this geometric information so that it is not required *a priori*. We also present results generated by the full hierarchical algorithm, which is a concatenation of these steps.

II. Mass and Center of Mass

The first stage in the processing estimates the mass and center of mass of the object. Consistency conditions for the Radon transform show that not all functions $g(t,\theta)$ are valid 2-D Radon transforms [5]. In particular, the two lowest order constraints show that the mass $m(\theta)$ of a projection must be equal to the mass m of the object, and the center of mass $c(\theta)$ of a projection

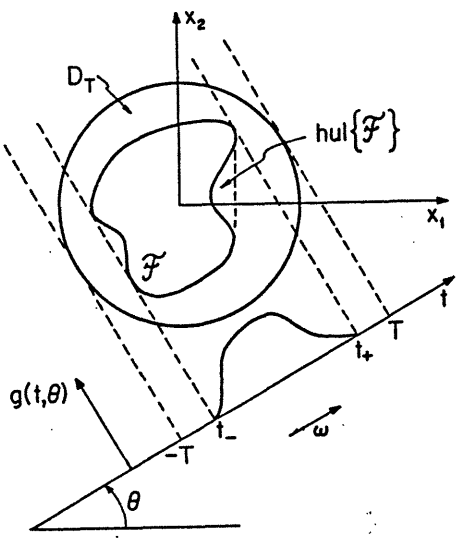

Fig. 1. Geometry of the 2-D Radon transform.

must be equal to the projection of the center of mass c of the object onto the ω-axis. Therefore, the *mass constraint* is

$$m(\theta) = \int_{-\infty}^{\infty} g(t,\theta)dt = m \tag{3}$$

and the *center of mass constraint* is

$$c(\theta) = \frac{1}{m}\int_{-\infty}^{\infty} tg(t,\theta)dt = c\cdot\omega\,. \tag{4}$$

These constraints may be used, together with the observed projections, to estimate the mass and center of mass of the object. We assume that the integral in (3) may be accurately approximated by a summation, so that the *observed mass* for the jth observed projection is given by

$$m_j = \frac{2T}{n_d}\sum_{i=1}^{n_d} y(t_i,\theta_j) = m + \frac{2T}{n_d}\sum_{i=1}^{n_d} n(t_i,\theta_j)\,. \tag{5}$$

Therefore, the observed masses are independent observations of the true mass m, observed in additive zero-mean white Gaussian noise. The ML estimate $\hat{m}$ of the true mass (which is also the minimum mean square error (MMSE) estimate) is just the average of the observed masses.

To estimate the center of mass, we use $\hat{m}$ in place of the true mass and approximate the integral of (4) by a summation. The *observed center of mass* is given by

$$\tilde{c}_j = \frac{1}{\hat{m}}\frac{2T}{n_d}\sum_{i=1}^{n_d} t_i y(t_i,\theta_j) \approx c_j + n_j \tag{6}$$

where c_j is the true center of mass of the jth observed projection. Then the system of equations $\tilde{c}_j = c\cdot\omega_j$ may be solved for the object's mass c using least squares, yielding an approximate ML or MMSE estimate $\hat{c}$.

Using the center of mass estimate, the projections may be shifted so that the center of mass of the object is centered. The new projections are given by

$$\tilde{y}(t,\theta) = y(t-\hat{c}\cdot\omega,\theta)\,. \tag{7}$$

This processing is required so that subsequent stages may assume the object to be centered at the origin.

III. Convex Support

The second stage in the hierarchical algorithm estimates the convex support of the object from the available projections. Fig. 1 shows that two support lines of the object determine a range of support for a projection, given by two *support values* t_- and t_+. If, on the other hand, one knows t_- and t_+ for all projections, this defines the convex support of the object. Unfortunately, this information is not readily available for two reasons: 1) we observe only a finite number of projections, and 2) the projections are observed in noise. A consequence of the first problem is that we may require additional prior information about the shape of expected objects in order to estimate the missing support values. A consequence of the second problem is that estimates of the lateral positions of any set of support lines may not be consistent with any object in the plane [6].

We approach convex support estimation in two stages. The first stage estimates the support positions within each projection and the second stage estimates a set of consistent support values for all observed and unobserved projections. In this section, we discuss two methods to accomplish the first stage; approaches to the second second step have been presented elsewhere [6].

Knot-Location Method

This method, based on the theory presented in [7], models each projection as a linear spline as shown in Fig. 2. The knots of interest reside at t_- and t_+, the support values of the projection. An observed projection may be treated as a time series and, in the range where t goes from $-T$ to the second knot, may be modeled by the following state and observation equations

$$x(i+1) = \begin{bmatrix} 1 & 2T/n_d \\ 0 & 1 \end{bmatrix} x(i) + \alpha \begin{bmatrix} 0 \\ 1 \end{bmatrix} \delta(i+1-k) \tag{8}$$

$$y(i) = \begin{bmatrix} 1 \\ 0 \end{bmatrix} x(i) + v(i)\,, \tag{9}$$

where $\delta(\cdot)$ is the discrete impulse function, α is the height of the discontinuity, k is the position of the first knot, and $v(i)$ is a sequence of independent zero-mean white Gaussian noise samples with variance σ^2.

The knot-location algorithm starts a Kalman filter at $t = -T$, assuming the above state-space description, and at each time instant it looks over a trailing window to estimate α at each point k in the window, assuming that the knot occurred at that point. When the generalized likelihood, calculated using the estimated $\hat{\alpha}$, is larger than a given threshold, a knot is deemed to have taken place and this value is declared as one support value of the projection. The other support value is found by running

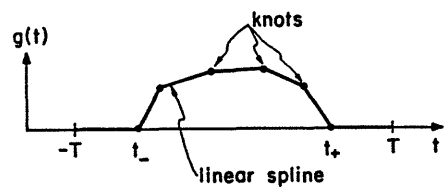

Fig. 2. Projection modeled as linear spline.

the knot-location algorithm backwards from $t = T$. More details of this algorithm may be found in [8].

Support-Width Penalty Method

The support-width penalty method uses the mass and center of mass of each projection as additional prior information as shown in Fig. 3. For every possible set of hypothesized support values, $\tilde{t}_-$ and $\tilde{t}_+$, the ML estimate $\hat{g}(t)$ of a complete projection is determined. Because of the mass and center of mass constraints and because of the assumed support values, the mass and center of mass of each projection is always correct, and the value of $\hat{g}(t)$ is zero outside the support values.

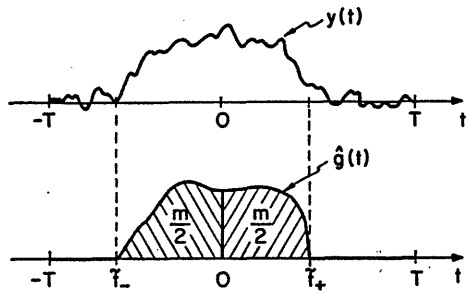

Fig. 3. Noisy projection and constrained estimate.

The goal is to choose the best support values given $\hat{g}(t)$ for all $\tilde{t}_-$ and $\tilde{t}_+$. Choosing the support values that maximize the likelihood is not adequate, since this procedure will nearly always pick $\hat{t}_- = -T$ and $\hat{t}_+ = T$. A support-width penalty is required, and the model order selection method due to Akaike [9] provides an information theoretic way to introduce this requirement.

Each half-projection is treated independently (see Fig. 3), and each left-hand half-projection is time-reversed for the calculation. Assuming that there are N samples in a half-projection and that the hypothesized support value is at index k, the ML estimate of the true half-projection is a vector $\hat{s}^k = [s_1^k, s_2^k, \ldots, s_N^k]^T$ that solves the quadratic program

$$\begin{aligned} \text{minimize} \quad & (y - s^k)^T (y - s^k) && (10) \\ \text{subject to} \quad & s_{k+1}^k = s_{k+2}^k = \cdots = s_N^k = 0, && \text{(Support)} \\ & s_i^k \geq 0 \ \ \forall i, && \text{(Positivity)} \\ & \frac{T}{n_d} s_0^k + \sum_{i=1}^{k} \frac{2T}{n_d} s_i^k = \frac{m}{2}. && \text{(Mass)} \end{aligned}$$

Akaike's method [9] adds a penalty term (based on the number of free parameters) to the likelihood function, specifying the Akaike Information Criterion (AIC). The Akaike estimate maximizes the AIC, yielding [8]

$$\hat{k} = \underset{0 \leq k \leq N}{\operatorname{argmin}} \frac{1}{\sigma^2} (y - \hat{s}^k)^T (y - \hat{s}^k) + 2k. \qquad (11)$$

This support estimate requires a line-search in k, with a quadratic program solved at each k. As k gets larger, the penalty term $2k$ begins to dominate so that the best support value estimate is not always N.

The support-width penalty method is of a quite different character than the knot-location method. In particular, the knot-location method uses derivative information to locate the change in slope in the projection over a local region. In contrast, the support-width penalty method uses the more global mass and center of mass information and, in fact, is very insensitive to small perturbations near the support value.

IV. Hierarchical Algorithm

A block diagram of the full hierarchical algorithm is shown in Fig. 4. The mass and center of mass estimation steps were discussed in Section II and support value estimation was discussed in Section III. The block labeled *Thresholds* derives thresholds for the knot-location method and is described in [8]. The *Support Vector* block takes the estimated support values and and produces a full estimate of the convex hull of the object as described in [6].

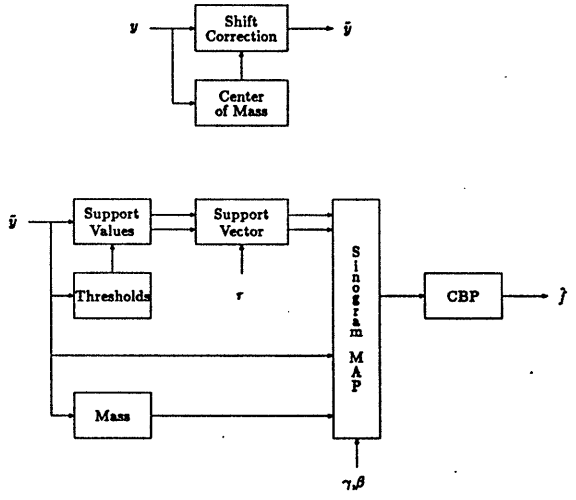

Fig. 4. Block diagram of hierarchical algorithm.

The *Sinogram MAP* block calculates the maximum *a posteriori* estimate of the full sinogram, incorporating convex support information and smoothness of the 2-D Radon transform, and assuming that the observed sinogram has been shift-corrected and normalized to unit mass. It solves a partial differential equation with constraints using an iterative primal-dual relaxation algorithm as describe in [2] and [8].

As shown in Fig. 4, the hierarchical algorithm requires three user inputs: r, γ, and β. These variables represent prior information about the shape of the convex hull of the object, the sinogram horizontal smoothness, and the sinogram vertical smoothness, respectively. They are coefficients of prior probabilities used in the various estimation stages, and may be empirically adjusted for different object classes or imaging geometries.

V. Experimental Results

Fig. 5a shows the 81 by 81 pixel M I T ellipse object used in the experiments of this section. An 81 by 60 noise-free sinogram, derived from an approximate strip-integration of an analytic representation of the M I T, is shown in Fig. 5b. The M I T ellipse object was chosen for experimentation because the loss of data over different angular regions affects the reconstructions in different ways. For example, the absence of line integrals parallel to the long axis of the ellipse causes a lack of information related to the narrow dimension of the ellipse, but retains information

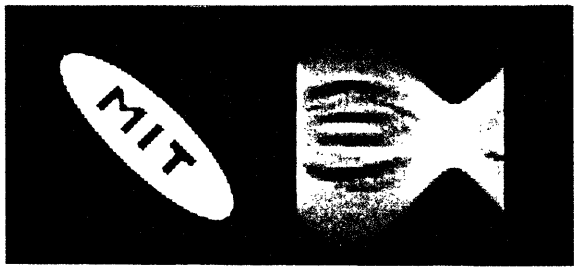

(a) (b)

Fig. 5. M I T ellipse and noise-free sinogram.

about the letters inside the ellipse. In contrast, the absence of line integrals parallel to the short axis of the ellipse obscures the letters, but reveals the narrowness of the ellipse.

Fig. 6 shows results from two limited-angle experiments. Figs. 6a–c are derived from an experiment that observes the leftmost 40 projections depicted in Fig. 5b with independent samples of zero-mean Gaussian noise added to each sample. The resulting data, having a signal to noise ratio (SNR) of 10dB, yields the image shown in Fig. 6a when reconstructed using convolution backprojection (CBP). A full sinogram MAP estimate, derived from the hierarchical algorithm, is shown in Fig. 6b with the estimated support values superposed on the image. Fig. 6c shows the reconstruction (using CBP) of Fig. 6b. Figs. 6d–f show an analogous sequence of images derived from an experiment that observes the rightmost 40 projections in noise, with SNR = 10dB as before.

These experiments use prior convex support information that assumes that objects tend to be circular. The use of this type of information is what allows interpolation of support information to the angles that are not observed. In the case of Figs. 6b and 6c, this information tends to cause the resulting object to be too circular, but the contrast between the object and its background and the clarity of the internal letters is clearly better than that in Fig. 6a. The support value interpolation of the convex hull is excellent in Figs. 6e and 6f and there is a dramatic improvement

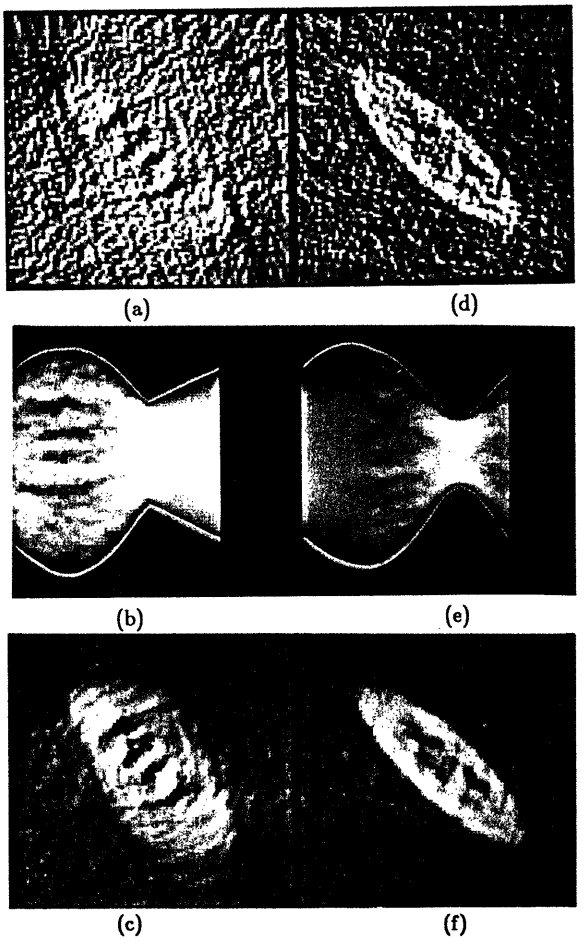

Fig. 6. Limited-angle experiments.

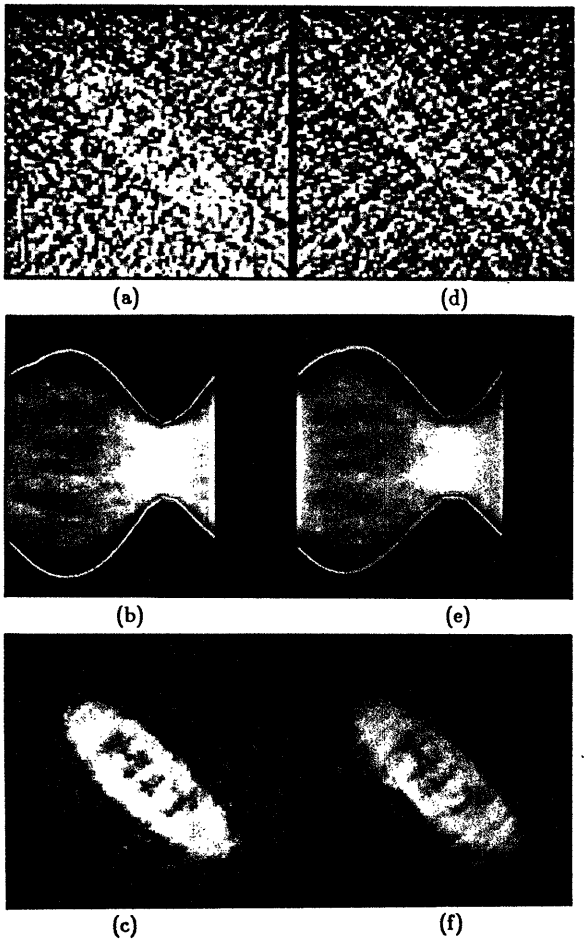

Fig. 7. Sparse-angle experiments.

in the object contrast. However, the lettering in the interior is only slightly more readable since this information is lost along with the 20 leftmost missing projections.

A similar set of experiments was conducted for sparse-angle cases, and the results are shown in Fig. 7. Figs. 7a–c are derived from a sparse angle experiment in which only 15 projections, evenly spaced in angle, are viewed in noise, with a 10dB SNR as before. Figs. 7d–f show an analogous set of images when only 10 evenly spaced projections are observed with the same SNR. Clearly, the sparse-angle cases better resolve, on balance, the detail of both convex hull and inner detail than the limited-angle cases. Also, in both sparse-angle cases, the improvement over CBP is quite evident — streak artifacts have disappeared, contrast is improved, and the legibility of the interior letters is greatly enhanced. However, circular swirling artifacts due to the horizontal smoothing effect have been introduced in both images.

VI. Discussion

We have demonstrated in this paper a method to estimate and hierarchically incorporate geometric information in a reconstruction algorithm designed for noisy and incomplete-data tomography. The method is based on estimation principles, incorporating prior probabilistic information and consistency conditions where needed to overcome problems resulting from insufficient data.

Acknowledgements

This research was supported by the National Science Foundation under grant ECS-87-00903 and the U.S. Army Research Office under grant DAAL03-86-K-0171.

References

[1] M. I. Sezan and H. Stark, "Image restoration by convex projections in the presence of noise," *Applied Optics*, vol. 22, no. 18, pp. 2781–2789, 1983.

[2] J. L. Prince and A. S. Willsky, "A projection-space map method for limited-angle reconstruction," in *Proceedings of the 1988 Int'l Conf. on Acoust. Sp. and Sig. Proc.*, 1988.

[3] G. T. Herman, *Image Reconstruction from Projections.* New York: Academic Press, 1980.

[4] J. A. Reeds and L. A. Shepp, "Limited angle reconstruction in tomography via squashing," *IEEE Trans. on Medical Imaging*, vol. MI-6, pp. 89–97, June 1987.

[5] D. Ludwig, "The Radon transform on Euclidean space," *Comm. Pure Appl. Math.*, vol. 19, pp. 49–81, 1966.

[6] J. L. Prince and A. S. Willsky, "Estimating convex shapes from support line measurements using prior geometric information," in *Proceedings of the Twenty-Sixth Annual Allerton Conf. on Comm., Control, and Comp.*, 1988.

[7] A. M. Mier-Muth and A. S. Willsky, "A sequential method for spline approximation with variable knots," Tech. Rep. ESL-P-759, M.I.T. Electronic Systems Laboratory, 1977.

[8] J. L. Prince, *Geometric Model-Based Estimation From Projections.* PhD thesis, Massachusetts Institute of Technology, 1988.

[9] H. Akaike, "Information theory and an extension of the maximum likelihood principle," in *2nd International Symposium on Information Theory*, 1972.